Electronic structure and optical properties of rutile RuO_2 from first principles*

Yang Ze-Jin(杨则金)[b], Guo Yun-Dong(郭云东)[a)†], Li Jin(李 劲)[b)c)], Liu Jin-Chao(刘锦超)[b)], Dai Wei(戴 伟)[b)d)], Cheng Xin-Lu(程新路)[b)], and Yang Xiang-Dong(杨向东)[b)]

[a)] *School of Physics and Electronic Information Engineering, Neijiang Normal University, Neijiang* 641112, *China*

[b)] *Institute of Atomic and Molecular Physics, Sichuan University, Chengdu* 610065, *China*

[c)] *College of Material and Chemical Engineering, Hainan University, Haikou* 570228, *China*

[d)] *Chinese Academy of Engineering Physics, Mianyang* 621900, *China*

(Received 10 October 2008; revised manuscript received 20 January 2010)

The systematic trends of electrionic structure and optical properties of rutile ($P4_2/mnm$) RuO_2 have been calculated by using the plane-wave norm-conserving pseudopotential density functional theory (DFT) method within the generalised gradient approximation (GGA) for the exchange–correlation potential. The obtained equilibrium structure parameters are in excellent agreement with the experimental data. The calculated bulk modulus and elastic constants are also in good agreement with the experimental data and available theoretical calculations. Analysis based on electronic structure and pseudogap reveals that the bonding nature in RuO_2 is a combination of covalent, ionic and metallic bonds. Based on a Kramers–Kronig analysis of the reflectivity, we have obtained the spectral dependence of the real and imaginary parts of the complex dielectric constant (ε_1 and ε_2, respectively) and the refractive index (n); and comparisons have shown that the theoretical results agree well with the experimental data as well. Meanwhile, we have also calculated the absorption coefficient, reflectivity index, electron energy loss function of RuO_2 for radiation up to 30 eV. As a result, the predicted reflectivity index is in good agreement with the experimental data at low energies.

Keywords: first principle, rutile RuO_2, electronic structure, optical property

PACC: 7125, 7890

1. Introduction

Attractions to investigate RuO_2 are due to its interesting fundamental properties[1−7] and its potential superhard characteristics.[2,3] The search for new superhard materials has been undertaken extensively during recent years.[8] A possible new class of hard materials has been suggested: the transition-metal dioxides containing heavy elements,[9] typically, the bulk modulus of pyrite RuO_2 was found to be 399 GPa,[10] which is the highest value reported in a material, except diamond that has a bulk modulus of 442 GPa.[11] Under ambient pressure, many MX_2 compounds take either the rutile ($P4_2/mnm$) or the $CaCl_2$ ($Pnnm$) structure,[12] between which the primary difference involves a rotation about the c axis of the MX_6 octahedra. Under usual conditions, RuO_2 has rutile structure,[10] and it transforms into a $CaCl_2$ structure at about 6 GPa[13] or 11.8 GPa,[14] and experiment shows that it transforms into a pyrite structure at about 12 GPa, while the theory reveals that $Pa\bar{3}$ structure can transform into an $fm\bar{3}m$ structure at about 89 GPa or 97 GPa.[3]

As far as the electronic structures are concerned, many efforts have been made to understand the internal atomic and electronic properties, e.g. a detailed study of electronic structure of RuO_2 has been reported by Glassford and Chelikowsky.[15] A full-potential linear muffin-tin orbital (FP-LMTO) calculation on the electronic structure and bulk modulus of fluorite RuO_2 has also been performed by Lundin *et al.*[16] Elastic properties of $Pa\bar{3}$ phase of RuO_2 have been investigated systematically by Tse *et al.*[3] The band structure, density of states and charge density of RuO_2 in rutile and orthorhombic ($CaCl_2$-type) structures have been researched by Benyahia *et al.*[17] Moreover, the Fermi surface of RuO_2 in rutile structure has been calculated on the basis of the self-consistent energy band structure in the local density approximation method.[18] In order to determine

*Project supported by the China Scholarship Council (CSC) and the National Natural Science Foundation of China (Grant Nos. 10676025 and 10574096), and the Science-Technology Foundation for Young Scientist of Sichuan Province, China (Grant No. 09ZQ026-049).

†Corresponding author. E-mail: g308yd@126.com

© 2010 Chinese Physical Society and IOP Publishing Ltd

electron-transport properties of RuO_2 in rutile structure, first-principles electronic-structure calculations have been done by Glassford and Chelikowsky.[19] In addition, the electronic and optical properties[20,21] and stabilisation of rutile RuO_2[2] have been described accurately by density functional theory. The Raman scattering observation of rutile-to-$CaCl_2$ phase transition, hardness and elasticity in cubic ruthenium dioxide[22] have been probed experimentally.

To study the superhard characteristics appropriately, a detailed description of the physical properties, such as the electronic, optical and elastic properties, is needed. Therefore, in this paper, first-principles calculations are used to investigate the electronic, optical and elastic properties of the rutile RuO_2. Since the transition-metal dioxides containing heavy elements have been suggested to be a possible new class of hard materials, it is helpful to explore the underlying relationship between the superhard characteristics and the properties in the transition-metal dioxides containing heavy elements.

2. Theoretical methods

In the present study, we have elaborated the electronic structure and optical properties of rutile RuO_2 via first principles calculation. Our calculations have been performed using the plane-wave pseudopotential density functional theory method given by the Cambridge Serial Total Energy Package (CASTEP) program.[23,24] In the electronic structure calculations, we have used the norm-conserving pseudopotential introduced by Hamann,[25,26] together with the revised Perdew–Burke–Ernzerhof (RPBE) of the generalised gradient approximation (GGA) exchange–correlation function.[27,28] Considering the computational cost, a plane-wave basis set with an energy cut-off 600.0 eV[3] has been applied, and the 12×12×12 Monkhorst–Pack mesh[29] has been used for the Brillouin-zone (BZ) k-point sampling. Pseudo atomic calculations have been performed for Ru ($4s^2 4p^6 4d^7 5s^1$) and O ($2s^2 2p^4$), where the self-consistent convergence of the total energy is at 5.0×10^{-7} eV/atom. It is found that these model parameters are sufficient in leading to well converged total energy and geometrical configurations.

The linear optical properties in solids can be described with the complex frequency-dependent dielectric function $\varepsilon(\omega) = \varepsilon_1(\omega) + \mathrm{i}\varepsilon_2(\omega)$. Since rutile RuO_2 compounds have tetragonal crystal structures, we need only to calculate one dielectric tensor component to characterise the linear optical properties completely. The imaginary or absorptive part $\varepsilon_2(\omega)$ of the frequency-dependent dielectric function is given by

$$\varepsilon_2(\omega) = \frac{e^2\hbar}{\pi m^2\omega^2}\sum_{\mathrm{v,c}}\int_{\mathrm{BZ}} |M_{\mathrm{vk}}(k)|^2\,\delta\left[\omega_{\mathrm{cv}}(k)-\omega\right]\mathrm{d}^3k. \tag{1}$$

The integral is carried out over the first Brillouin zone, and the momentum dipole elements $M_{\mathrm{vk}}(k) = \langle U_{\mathrm{cv}}\,|\boldsymbol{e}\cdot\nabla|\,U_{\mathrm{ck}}\rangle$, where $\boldsymbol{e}$ is the potential vector defining the electric field, are matrix elements for direct transitions between valence-band $u_{\mathrm{vk}}(r)$ and conduction band $u_{\mathrm{ck}}(r)$ states, and $h\omega_{\mathrm{cv}}(r) = E_{\mathrm{ck}} - E_{\mathrm{vk}}$ is the corresponding transition energy.

The real part $\varepsilon_1(\omega)$ of the frequency-dependent dielectric function can be derived from the imaginary part using the Kramers–Kronig relation

$$\varepsilon_1(\omega) = 1 + \frac{2}{\pi}p\int_0^\infty \frac{\omega'\varepsilon_2(\omega')}{\omega'^2-\omega^2}\mathrm{d}\omega', \tag{2}$$

where p denotes the Cauchy principal value of the integral. Based on the knowledge of both real and imaginary parts of the frequency-dependent dielectric function, we can calculate the important optical functions such as the refractive index $n(\omega)$

$$n(\omega) = \left[\frac{\varepsilon_1(\omega)}{2} + \frac{\sqrt{\varepsilon_1(\omega)+\varepsilon_2(\omega)}}{2}\right]^{1/2}. \tag{3}$$

In this work, we estimate the absorption coefficient $\alpha(\omega)$, the reflectivity coefficient $R(\omega)$, and the extinction coefficient $k(\omega)$ in the following forms:

$$N(\omega) = n(\omega) + \mathrm{i}k(\omega), \tag{4}$$

$$N(\omega) = n(\omega) + \mathrm{i}k(\omega), \tag{5}$$

$$N^2(\omega) = \varepsilon_1(\omega) + \mathrm{i}\varepsilon_2(\omega), \tag{6}$$

$$R(\omega) = \left|(1-N)/(1+N)\right|^2, \tag{7}$$

where N is the complex refractive index, and the imaginary part $k(\omega)$ is related to the absorption coefficient by $\alpha(\omega) = 2k\omega/c$.

3. Results and discussion

The obtained equilibrium structure under ambient conditions is listed in Table 1, together with the experimental data[30−34] and available theoretical results.[3,15,17,35]

Table 1. The calculated equilibrium structure parameters (in unit of Å, 1 Å = 0.1 nm), aggregate elastic modulus (GPa) and elastic constants (GPa) of rutile RuO_2 at 0 GPa and 0 K.

	a	c	u	B_0	c_{11}	c_{33}	c_{44}	c_{66}	c_{12}	c_{13}
GGA	4.5149	3.1156	0.3057	245.56	308.38	508.95	108.63	208.22	214.49	171.05
Exp[30]	4.4999		0.3056							
Exp[31]		3.111								
Exp[32]	4.49307	3.10639	0.3056	270						
Exp[33]	4.492	3.106	0.3058							
Exp[34]				249						
Ref. [3]LDA	4.474	3.092	0.3058	313/299						
Ref. [3]GGA	4.554	3.137	0.3054	260.5						
Ref. [15]	4.56	3.16	0.3068	284						
Ref. [17]LDA	4.433	3.09		335.68						
Ref. [17]GGA	4.543	3.126		292.8						
Ref. [35]	4.497	3.0984	0.3061	260.1	309.7	569.3	124	236.7	235.2	198.4

It is obvious that our calculations are in excellent agreement with experimental data. According to the generalised elastic stability criteria,[36] it is certain that rutile RuO_2 structure is elastically stable under ambient conditions. Furthermore, both the large c_{33}/c_{11} and small c_{13}/c_{12} values indicate that atomic bonding along the c-axis is stronger than the one along the a-axis, which is consistent with the fact that the bulk modulus B is larger than shear modulus G (109.86 GPa) under ambient pressure. At the same time, the fact that the mechanical anisotropy bulk modulus in c-axis (793.85 GPa) is larger than in a-axis (715.48 GPa) also indicates that the interatomic bonds along the c-axis are stronger than the bonds along the a-axis, which is consistent with the fact of $c_{33} > c_{11}$.

It is interesting to note that there is a substantial difference between c_{44} and c_{66} values, indicating the anisotropic character of atomic bonding between adjacent planes in different directions. In rutile RuO_2, the shear anisotropy factor for the [101] shear direction, $A_1 = 4c_{44}/(c_{11} + c_{33} - 2c_{13}) = 0.9143$, is smaller than that for the [110] direction, $A_2 = 2c_{66}/(c_{11} - c_{12}) = 4.4354$. The small A_1 value is indicative of the weak cohesion between Ru and O layers. Based on the linear elasticity approximation, the compressibilities χ_a and χ_c along the a and c directions have been calculated from the elastic constants respectively. Obtained values $\chi_a = 1.6268 \times 10^{-3}$ GPa^{-1} and $\chi_c = 0.8703 \times 10^{-3}$ GPa^{-1} show a big anisotropy between a and c directions.

It is well known that the Cauchy relation $c_{12} = c_{66}$ and $c_{13} = c_{44}$ should be satisfied when interatomic potentials are purely central. The deviations of the Cauchy relations, $\delta = c_{12} - c_{66}$ and $\delta = c_{13} - c_{44}$, are a measure of the contribution from the noncentral many-body force. Thus, the small $\delta = c_{12} - c_{66}$ (6.27) and large $\delta = c_{13} - c_{44}$ (62.42) values indicate that the noncentral many-body force is different in different directions.

According to the high symmetry lines in the Brillouin zone, the valence bands and the conduction bands are presented at 0 K and 0 GPa. The valence band maximum occurs at the axis of G–X which is higher than the Fermi level, and the conduction band minimum occurs at X point which is lower than the Fermi level; this means that there exists a pseudogap. The pseudogap can still be found in pyrite RuO_2, however, it cannot be found in fluorite RuO_2.[3] At the same time, the band structure of rutile RuO_2 also shows strong metallic properties.

In Fig. 1 we present the density of states (DOS) calculated by GGA, and the Fermi energy is taken to be zero. The O 2s band is located approximately at –17.65 eV which is slightly higher than that in pyrite and fluorite RuO_2.[17,18] The valence band width is about 3 eV, which is larger than that of rutile RuO_2[17] with a width of 2.5 eV, and is also larger than that in $CaCl_2$ RuO_2[17] with a width of 1.4 eV, whereas it is smaller than that in pyrite RuO_2 with a width of 4 eV. The valence band width below the Fermi level of O 2p is 7.7 eV which is larger than in rutile RuO_2 with a width of 5.9 eV or 6.8 eV,[18] whereas it is lower than that in fluorite RuO_2[17] with a width of 8.0 eV, and is also lower than that in pyrite RuO_2 with a width of 10.12 eV. The obtained O 2p band edge is

located at around –8.5 eV. Both the band width and the band edge are in agreement with the photoelectron spectroscopy measurements (XPS), which show a bandwidth of nearly 7 eV and the edge located at around –9 eV.[37,38] This pseudopotential results agree well with theoretical results,[20] having a bandwidth of 6.7 eV and band edge of –8.5 eV which have been obtained by using full-potential linearized augmented plane wave method. The conduction band width is about 6.29 eV, which is slightly lower than that of pyrite RuO_2 with a value of 6.74 eV, and is larger than that of fluorite RuO_2 with a value of 3 eV. The total DOS contributed by the O 2p density at the Fermi level is 0.28, which is far greater than that of fluorite RuO_2 (below 0.05)[18] and far smaller than that of pyrite RuO_2 (1.86), and the contributions of the Ru 4d electron are 0.98 which is smaller than that of fluorite RuO_2 (below 1.3) and pyrite RuO_2 (about 4.6). The bottom of the Ru 4d manifold is located approximately at –1.9 eV which is consistent with that in pyrite RuO_2 (–1.95 eV) and fluorite RuO_2 (−1.8 eV), and the intensity of rutile RuO_2 is 0.11, which is smaller than that of pyrite RuO_2 (0.65) but larger than that of fluorite RuO_2 (0.04). The main peak at –0.8 eV is the same as in fluorite RuO_2 but lower than that of pyrite RuO_2 (–0.6 eV). The rutile peak value is 7.2 which is lower than pyrite peak, the corresponding value being 11.55 but larger than fluorite RuO_2 peak the corresponding value being 3.05, and our results give a small shift compared with rutile values,[18] corresponding to –1.5 eV and –0.7 eV, respectively. The conduction band bottom of the Ru 4d manifold is located at 1.55 eV with the intensity of 0.21 which is consistent with that in pyrite RuO_2, corresponding to 1.5 eV with 0.27. The conduction band bottom in fluorite RuO_2, however, is located at 0.36 eV with an intensity of 0.18. The Fermi energy level shows sharp peaks, characters of which are contributed predominantly by the O 2p and Ru 4d electron densities, as is different from the rutile DOS[18] and fluorite RuO_2.[3] It is found that Ru 4d and O 2p states overlap completely from –10 eV to 5 eV, which is evidently indicative of a covalent interaction between them, resulting from strong hybridization.

The DOS of rutile RuO_2 possesses greater value (3.2) than that of fluorite RuO_2 (1.8), but is lower than that of pyrite RuO_2 (6.4) at the Fermi level, which indicates a moderate metallic feature of rutile RuO_2 in its crystalline state. The nearly free-electron states of the Ru 5s are the principal cause for metallicity of RuO_2.

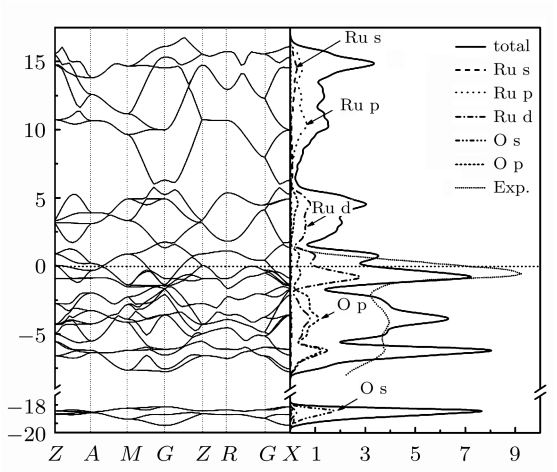


Fig. 1. Energy band structure at the high symmetry points in the Brillouin zone and the density of states of rutile RuO_2. Results are compared with the experimental results given in Ref. [38].

In the rutile structure each metal atom Ru is surrounded by a nearly octahedral array of six oxygen atoms, and therefore the fivefold-degenerate d states split into partially occupied triply degenerate t_{2g} and unoccupied doubly degenerate e_g states. As a result, the Fermi energy is near the minimum of the t_{2g} manifold, showing a metallic feature. The low DOS at the Fermi level is responsible for the stabilisation of the structure, where the rutile level is higher than the counterpart in fluorite phase, and the Fermi level falls in a sharp peak, leading to a structural phase transformation induced by pressure.

Although there is a large hybridization between Ru 4d and O 2p states, the charge transfer from Ru to O is nonnegligible in the present case. From the Mulliken population results, it is also found that the charge transfer is as large as about 1.16 electrons, which are slightly larger than that in pyrite (1.02) or in fluorite (1.01), and the transfer shows weak pressure dependence. Therefore, the bonding behaviour between Ru–O has ionic nature owing to charge transfer. In a word, the results show that the bonding nature in RuO_2 is due to a combination of covalent, ionic and metallic characteristics.

The theoretical DOS function is compared to the XPS measurements[38] in Fig. 1. With the location of the experimental peak coincident with the theoretical one, the spectra are in a reasonable agreement. Because of the experimental broadening it is not possible to determine precisely the band width suggested by the XPS measurement. However, judging by the spectrum in Fig. 1, the valence band width consisting

of O 2p and Ru 4d agrees well with the XPS measurements, and the conduction band width is lower than the present theoretical results by 4.0 eV. In spite of the fact that the width of the O 2p and Ru 4d in the present calculation is in agreement with the XPS measurement, the comparison between the measured and the calculated results suggests that our total DOS is slightly underestimated at the Fermi level and overestimated in the valence band, as is similar with the case of the *ab initio* calculations.[39,40] The slight deviation in values of the theoretical DOS at the Fermi level from experimental measurement is because of the complicated bonding nature of the transition metal Ru 4d and O 2p electrons.

The optical properties are studied through the absorption coefficient, reflectivity, energy loss function, refractivity index, dielectric function and conductivity index at the equilibrium lattice constant and the results are compared to the experimental data.[41] The calculated optical properties at the equilibrium lattice constant have been presented in Figs. 2 and 3, for the energy range up to 30 eV. In order to account for the structures observed in the optical spectra, it is customary to consider transitions from occupied to unoccupied bands in the electronic energy band structure, especially at high symmetry points in the Brilllouin zone.

The calculated linear absorption spectrum is displayed in Fig. 2(a). The absorption edge starts from about 0 eV, corresponding to the energy pseudogap. The rutile RuO_2 has an absorption band from 0 to 23 eV, which contains eight main peaks for $E\perp c$ and seven main peaks for $E//c$. In the high energy region (above 23 eV), the crystal is transparent because it progressively becomes more difficult for the electrons to respond. The shapes and the intensities of the two absorption spectra are similar and comparable at these photon energies of 0–23 eV.

The theoretical spectra of the electron energy loss function are shown in Fig. 2(b). The electron energy loss function $L(\omega)$ is an important factor for describing the energy loss of a fast electron traversing in a material, which is the imaginary part of the reciprocal of the complex dielectric function. The prominent peaks in $L(\omega)$ spectra represent the characteristic associated with the plasma resonance, and the corresponding frequency is the so-called plasma frequency $\omega_{\rm p}$, above which the material is a dielectric $[\varepsilon_1(\omega) > 0]$ and below which the material behaves like a metallic compound in some sense $[\varepsilon_1(\omega) < 0]$. The peaks of $L(\omega)$ correspond to the trailing edges in the reflection spectra, and the prominent peaks of $L(\omega)$ are situated at energies corresponding to the abrupt reductions of $R(\omega)$. The $E\perp c$ peak of $L(\omega)$ is at 22.85 eV corresponding to the intensity 11.85, whereas the $E//c$ peak is at 22.27 eV corresponding to the intensity 15.85. The peak intensity shows the direction dependence and the anisotropy of the material. The wide range of energy loss is in agreement with the feature of $\varepsilon_1(\omega)$ shown in Fig. 2(c), because wide range $[\varepsilon_1(\omega) < 0]$ regions exist for the two polarisations.

The reflectivity for the light polarisations $E\perp c$ and $E//c$ are compared to the experimental data in Fig. 2(c). Our reflectivity curves are in good quantitative agreement with the measured spectra up to $\hbar\omega = 2.5$ eV. For photon energies above 2.5 eV the experimental structures are too weak to establish a reliable correspondence with the theory. The reflectivity spectrum of the rutile RuO_2 shows some peaks which can be interpreted as the interband transitions from the valence to conduction band.

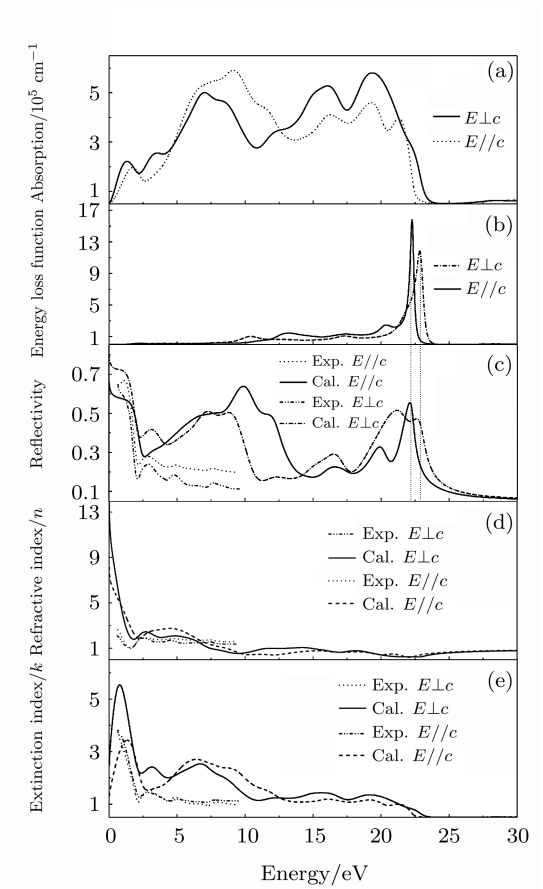


Fig. 2. (a) The calculated absorption coefficient $\alpha(\omega)$, (b) electron energy loss spectrum $L(\omega)$, (c) optical reflectivity spectrum $R(\omega)$, (d) refractive index $n(\omega)$, (e) extinction coefficient $k(\omega)$ of rutile RuO_2. Results are compared with the experimental data in Ref. [41].

The refractive index and the extinction coefficient are displayed in Figs. 2(d) and 2(e), respectively. The static refractive index $n(0)$ is found to have the value 13.93 for $E\perp c$ and 8.13 for $E//c$. They decrease with energy in the transparency region, reaching a local minimum at 1.8 eV for $E\perp c$ and 2.4 eV for $E//c$. The extinction coefficient $k(\omega)$ increases with energy in the transparency region, reaching the peaks in the ultraviolet at about 0.78 eV for $E\perp c$ and 1.33 eV for $E\perp c$. It then decreases to a local minimum level at 2.36 eV $E\perp c$ and 2.85 eV $E//c$. The local minimum of the extinction coefficient $k(\omega)$ corresponds to the local minimum of refractive index $n(\omega)$ at around 2.5 eV.

The calculated real part and imaginary part of the conductivity index are shown in Fig. 3(a), from which we can see that it corresponds well to the variation of imaginary part of the dielectric function. Figures 3(b) and 3(c) show the imaginary and real parts of the dielectric function for rutile RuO_2 respectively. As seen in Fig. 2 (b), the $\varepsilon_2(\omega)$ spectra have a high absorption below 2 eV, which is due to transitions within Ru t_{2g} bands while the other optical structures above 2 eV arise from p–d electronic transitions. In the energy range of 0.83–2.04 eV of Fig. 2(c), the intraband transitions play an important role and the large negative values $\varepsilon_1(\omega)$ for the $E\perp c$ components indicate that the crystal has a Drude-like behaviour, whereas it is not the case for the $E//c$ component. At higher energies, the optical features are due to electronic transitions from oxygen 2p to metal d bands. For $E\perp c$, the absorptive part of the dielectric function $\varepsilon_2(\omega)$ exhibits a main peak, with a magnitude of 55.23, which is located at about 0.01 eV. For $E//c$, the absorptive part of the dielectric function $\varepsilon_2(\omega)$ exhibits a main weak peak, with a magnitude of 25.33, which is located at about 0.82 eV. Comparison between the measured and calculated spectra shows that the theory tends to overestimate the dielectric function in the low energy regime and underestimate it for high photon energies. The static dielectric constant $\varepsilon_2(0)$, calculated at the equilibrium lattice constant is about 55.23. Nevertheless, compared with the experimental dielectric function, the structures in the energy range of 1–3 eV in $\varepsilon_1(\omega)$ and $\varepsilon_2(\omega)$, the refractive index and reflectivity curves seem to have their counterparts in the experimental spectra.

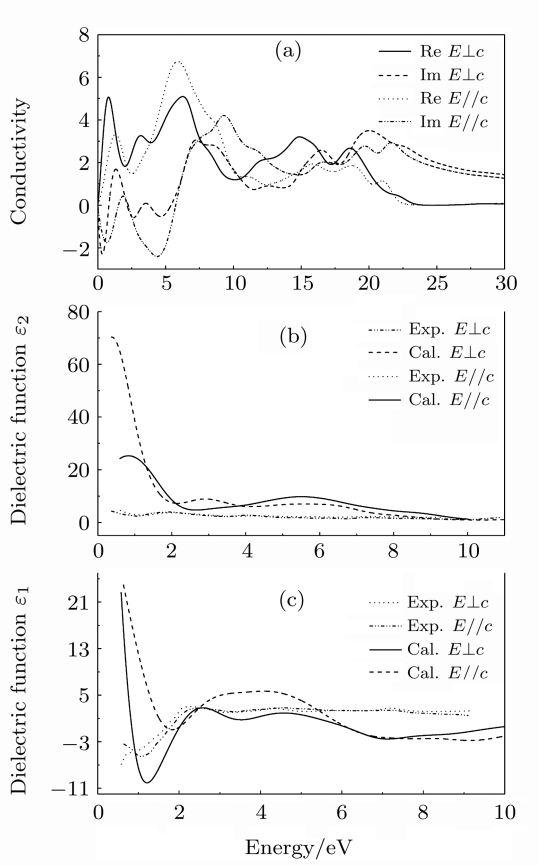


Fig. 3. (a) The calculated real part and imaginary part of the conductivity index, (b) imaginary part $\varepsilon_2(\omega)$, (c) real part $\varepsilon_1(\omega)$ of the dielectric function of rutile RuO_2. Results are compared with the experimental data in Ref. [41].

4. Conclusions

We have performed the comprehensive elastic, electronic structure and optical investigation of the rutile RuO_2. The obtained equilibrium structure, elastic constants and bulk modulus of rutile RuO_2 are in good agreement with the experimental data and available theoretical calculations. Our calculations reveal that the rutile phase shows elastic anisotropy and elastic stability under ambient conditions. The calculated band structure and DOS show that the bonding nature in RuO_2 is a combination of covalent, ionic and metallic bonds, and that the theoretical DOS agrees well with the experimental data. The dielectric function and optical properties are presented in a wide energy range between 0 and 30 eV, and they agree well with the experimental data.

References

[1] Goodenough J B In: Reiss H (Ed.) 1971 *Progress in Solid-State Chemistry* Vol.5 (Oxford: Pergamon)

[2] Hugosson H W, Grechnev G E, Ahuja R, Helmersson U, Sa L and Eriksson O 2002 *Phys. Rev.* B **66** 174111

[3] Tse J S, Klug D D, Uehara K, Li Z Q, Haines J and Léger J M 2000 *Phys. Rev.* B **61** 10029

[4] Yang Z J, Guo Y D, Wang G Ch, Li J, Dai W, Liu J Ch, Cheng X L and Yang X D 2009 *Chin. Phys.* B **18** 4981

[5] Sakata T, Kawai T and Hashimoto K 1982 *Chem. Phys. Lett.* **88** 50

[6] Shafer M V and Armstrong J 1978 *IBM Tech. Discl. Bull.* **20** 4633

[7] Pedder J D 1976 *Science Technol.* (USA) **2** 259

[8] Leger J M and Haines J 1997 *Endeavour.* **27** 121

[9] Leger J M, Haines J and Blanzat B 1994 *J. Mater. Sci. Lett.* **13** 1688

[10] Haines J, Leger J M and Shulte O 1996 *Science.* **271** 629

[11] Huntington J B In: Seitz F and Turnbull D 1958 *Solid State Physics* Vol.7 (New York: Academic)

[12] Burdett J K 1985 *Inorg. Chem.* **24** 2244

[13] Haines J and Léger J M 1993 *Phys. Rev.* B **48** 13344

[14] Rosenblum S S, Weber W H and Chamberland B L 1997 *Phys. Rev.* B **56** 529

[15] Glassford K M and Chelikowsky J R 1993 *Phys. Rev.* B **47** 1732

[16] Lundin U, Fast L, Nordström L, Johansson B, Wills J M and Eriksson O 1998 *Phys. Rev.* B **57** 4979

[17] Benyahia K, Nabi Z, Tadjer A and Khalfi A 2003 *Physica* B **339** 1

[18] Yavorsky B Yu, Krasovska O V, Krasovskii E E, Yaresko A N and Antonov V N 1996 *Physica* B **225** 243

[19] Glassford K M and Chelikowsky J R 1994 *Phys. Rev.* B **49** 7107

[20] de Almeida J S and Ahuja R 2006 *Phys. Rev.* B **73** 165102

[21] Daniels R R, Margaritondo G, Georg C A and Lévy F 1984 *Phys. Rev.* B **29** 1813

[22] Léger J M, Djemia P, Ganot F, Haines J, Pereira A S and Jormada J A H 2001 *Appl. Phys. Lett.* **79** 2169

[23] Payne M C, Teter M P, Allen D C, Arias T A and Joannopoulos J D 1992 *Rev. Mod. Phys.* **64** 1045

[24] Milman V, Winkler B, White A, Packard C J, Payne M C, Akhmatskaya E V and Nobes R H 2000 *Int. J. Quantum. Chem.* **77** 895

[25] Hamann D R, Schlüter M and Chiang C 1979 *Phys. Rev. Lett.* **43** 1494

[26] Bachelet G B, Hamann D R and Schlüter M 1982 *Phys. Rev.* B **26** 4199

[27] Perdew J P, Burke K and Ernzerhof M 1996 *Phys. Rev. Lett.* **77** 3865

[28] Hammer B, Hansen L B and Norskov J K 1999 *Phys. Rev.* B **59** 7413

[29] Monkhorst H J and Pack J D 1976 *Phys. Rev.* B **13** 5188

[30] Meade C and Jeanloz R 1990 *Rev. Sci. Instrum.* **61** 2571

[31] Tsuchida Y and Yagi T 1989 *Nature* (London) **340** 217

[32] Xu J H, Jarlborg T and Freeman A J 1989 *Phys. Rev.* B **40** 7939

[33] Haines J, Léger J M, Schulte O and Hull S 1997 *Acta Crystallogr., Sect.* B: *Struct. Sci.* **53** 880

[34] Boman C E 1970 *Acta Chem. Scand.* **24** 116

[35] Grillo M E 2004 *Phys. Rev.* B **70** 184115

[36] Wallace D C 1992 *Thermodynamics of Crystals* (New York: Wiley) Chap.1

[37] Kötz R and Stucki S 1986 *Electrochim. Acta* **31** 1311

[38] Riga J, Tenret-Noël C, Pireaux J J, Caudano R, Verbist J J and Gobillon Y 1977 *Phys. Scr.* **16** 351

[39] Krasovska O V, Krasovskii E E and Antonov V N 1995 *Phys. Rev.* B **52** 11825

[40] Guan L, Liu B T, Li X, Zhao Q X, Wang Y L, Guo J X and Wang S B 2008 *Acta Phys. Sin.* **57** 482 (in Chinese)

[41] Goel A K, Skorinko G and Pollak F H 1981 *Phys. Rev.* B **24** 7342